THE ANNALS OF "DUNAREA DE JOS" UNIVERSITY OF GALATI.
FASCICLE IX. METALLURGY AND MATERIALS SCIENCE
N^0. 3 – 2011, ISSN 1453 – 083X

A COMPARATIVE APPROACH OF DEGRADATIVE POTENTIAL OF TWO DIFFERENT NANOPHOTOCATALYSTS ONTO A MODEL TEXTILE DYE

Diana TANASA[1], Narcisa VRINCEANU[1], Claudia-Mihaela HRISTODOR[1], Eveline POPOVICI[1], Diana COMAN[2], Florin BRINZA[1], Ionut Lucian BISTRICIANU[3], Daniela Lucia CHICET[3]
[1]"Al.I. Cuza" University, Iasi,
[2]„Lucian Blaga" University from Sibiu,
[3]„Gh. Asachi" Technical University
email: narcisa.vrinceanu@ulbsibiu.ro

ABSTRACT

Motivations and objectives. *It is quite a difficult issue to treat, decolorize and mineralize textile dye waste containing dyes by conventional chemical methods (primary: adsorption, flocculation and secondary: chlorination, ozonization. It has been demonstrated that semiconductor photocatalytic oxidation of organic substances can be an alternative to conventional methods of removal of organic pollutants from water [1]. Advanced oxidation processes (AOPs) employing heterogeneous catalysis have emerged as a potentially destructive technology leading to the total mineralization of most of organic pollutants. An additional advantage of the photocatalytic process is its mild operating conditions and the fact the semiconductor can be activated by sunlight (near UV), thus reducing significantly the electric power requirement and hence the operating cost [2].*

The main result and characterizing aspect *of the research consist of the effectiveness of a semiconductor photocatalytic treatment of synthetic wastewater. Nanophotocatalysts ZnO have been successfully grown by hydrothermal method, onto some fibrous supports previously functionalized (grafted with MCT (monochlorotriazinyl-β-cyclodextrin, MCT-β-CD). The synthesis is reported elsewhere. The hydrothermal synthesis was performed using two types of surfactants widely used in nanoparticles preparation: Pluronic P123(triblock copolymer) and CTAB (cetyltrimethylammonium bromide). The novelty of the study consists in using these two different surfactants in growning of ZnO onto the fibrous supports. For degradation of Erionyl Roth dye, batch experiments were performed by irradiating the aqueous solution of model textile dye, containing ZnO nano-coated fibrous supports as semiconductor, in the presence of UV light. The photocatalytic process occurs under the illumination of an UV lamp, emitting light at wavelength 365 nm. The rate of decolorization was estimated spectrophotometrically from residual concentrations.*

Results and discussion. *The enhancement of the photocatalytic activity is attributed to the CTAB. The performance of the photocatalytic system indicated that the photodegradation of the Erionyl Roth, in the presence of CTAB, occured with a 20 % reduction of time, compared to P123.The study has demonstrated that using the semiconductor performed by CTAB on the ZnO nano-oxides synthesized onto previously MCT grafted fibrous supports is effective in degradation of dyes as well as in the treatment of textile dye waste.*

KEYWORDS: fibrous linen nanocomposites, photodegradation, nanophotocatalyst, zinc oxide

1. Introduction

Generally present in the effluents of the textile, cosmetics, paper, leather, pharmaceutical, food and other industries, dyes are among the most important water pollutants. There are many methods (coagulating sedimentation, filtration, electro-coagulation, and adsorption by activated carbon) which have been investigated to remove the dyes; the main disadvantage of these methods consists in only transferring the dyes from one medium to another. Consequently, the developing of environmentally benign routes combining effective adsorption with enhanced photocatalytic efficiency, which completely mineralizes the organic pollutants became crucial [1,2]. Due to advances in its synthesis and unique optoelectronic, catalytic, and photochemical properties, ZnO, a compound semiconductor with a band gap of 3.37 eV, has attracted substantial attention in recent years. Although TiO_2 has been widely used as the most active photocatalyst[3,4], ZnO could be a suitable alternative because of its lower cost, larger quantum yields, and better antibacterial effect. ZnO has been successfully used in photocatalytic degradation of pollutants [5,6] and is more efficient in the decomposition of several organic contaminants than TiO_2 [2,7,8]. However, ZnO nanoparticles are prone to aggregation especially after calcination above 400◦C. This results in a remarkably reduced surface area and much larger crystallite size. In addition, ZnO has a relatively low adsorptive capacity, and its photocatalytic efficiency is not high in very dilute solutions of organic pollutants. Consequently, enrichment of reactants by adsorption is required for a highly efficient photocatalytic performance [9-11].

Recently green chemistry and chemical processes have emphasized the preparation of nanoparticles to eliminate or minimize generated waste and implement sustainable processes [12]. Nanoparticles of metal oxide and sulfides are prepared with polysaccharides as stabilizer. Zinc oxide nanoparticles can be synthesized using water as a solvent and MCT-β-CD(MonoChlorotriazinyl–β-Cyclodextrin) as a stabilizer [13,14,15].

2. Experimental approach

2.1. Synthesis of nano-ZnO particles

In our research ZnO nanoparticles were synthesized *in-situ* on linen fibrous supports having a certain concentration of MCT-β-CD (monochlorotriazinyl– β -cyclodextrin) by using the hydrothermal method. The linen samples with sizes of 30 x 30 cm^2 were immersed in the solution prepared as follows: zinc acetate $Zn(CH_3COO)_2{\cdot}2H_2O$, purity – 99%) (0,005 mol) as precursor was solved in deionized water to form a clear solution by stirring and then 0,1 mol of urea solution was added drop-wise with constant stirring. Second, the pH value of the mixed solution was adjusted to 5 by adding acetic acid, added drop wise. The final reaction mixture was then magnetically stirred for two hours at room temperature and poured into into stainless-steel autoclaves with a 100-ml Teflon (poly[tetrafluoroethylene]), followed by immersion of the fibrous supports. Then the autoclaves were placed in the oven for the hydrothermal treatment at 90◦C overnight.

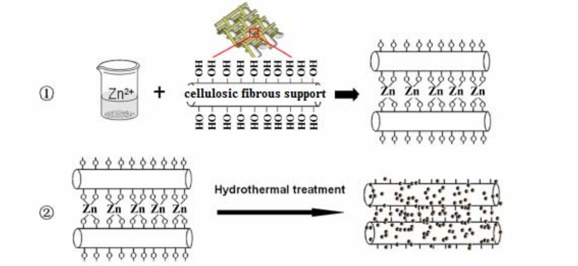

Fig. 1. *Flow chart for the preparation of nanoparticles-coated linen support.*

The autoclaves have been cooled down to room temperature naturally. The textile samples are then extracted from the autoclaves. The obtained products were washed several times with distilled water. After complete washing nanocomposites were dried at 60◦C overnight for 3 h for complete conversion of the remaining zinc hydroxide to zinc oxide.

2.2. Photocatalytic activity of the synthesized catalysts

The photocatalytic experiments were conducted in a 400 ml beaker under the illumination of a single UV light lamp produced by Vilber Lourmat France, which predominantly emits at 365nm with intensity of 350 μW/cm^2. Erionyl Roth was provided by a certain textile enterprise. All aqueous solutions were prepared using deionised water. For each experiment, the reaction suspension was prepared by adding 0.3 mg catalyst into 150 mL Erionyl Roth solution with an initial concentration of 30 mg/L. The suspension was magnetically stirred for 30 minutes in the dark to ensure the absorption/desorption equilibrium between dye molecules and the photocatalyst surface. Afterwards, the suspension was irradiated by the UV lamp. During the photodegradation process, the UV lamp was positioned horizontally above the surface of the suspension. In all experiments, the reaction temperature was kept at 25 ±2ºC.

Samples were taken out for measurement after various reaction times. The upper clear liquid obtained after centrifugal separation was analyzed by UV-Vis spectroscopy, on a Shimadzu UV-2401 UV-

Vis spectrophotometer. The maximum absorbance of the Erionyl Roth was found at 516 nm, and the concentration of the solutions has been determined using the calibration curve.

2.3. Instrumentation for characterization of ZnO–MCT-B-CD (Monochlorotriazinyl– β -Cyclodextrin) grafted linen fibrous nanocomposites

The phase and the microstructure of the samples were characterized by using X-ray diffraction and scanning electron microscopy-EDX, humidity (water vapors) sorption measurement/ humidity sorption/desorption.

2.3.1. Scanning electron microscopy (SEM)

Scanning Electron Microscope (SEM) images of the samples were obtained from a Quanta 200 3D Dual Beam type microscope from FEI Holland.

2.3.2. X-ray diffractometry

The ZnO–MCT-β-CD Monochlorotriazinyl–β-Cyclodextrin) powders were tightly packed into the sample holder. X-ray Diffraction (XRD) data for structural characterization of the various prepared samples of ZnO were collected on an X-ray diffractometer (PW1710) using Cu-Kα radiation (k = 1.54 Å) source (applied voltage 40 kV, current 40 mA). About 0.5 g of the dried particles were deposited as randomly oriented powder onto a Plexiglass sample container, and the XRD patterns were recorded at angles between 20° and 80°, with a scan rate of 1.5°/min. Radiation was detected with a proportional detector.

2.3.3. FTIR spectroscopy

FTIR was used to examine changes in the molecular structures of the samples. Analysis has been recorded on a FTIR JASCO 660+ spectrometer. The analysis of the studied samples was performed at 2 cm^{-1} resolution in transmission mode. Typically, 64 scans were signal averaged to reduce spectral noise.

3. Results and discussion

3.1. Characterization of ZnO–linen fibrous supports nanocomposites

SEM images below belong to linen support, non-functionalized (non-grafted), without hydrothermal treatment under different magnifications.

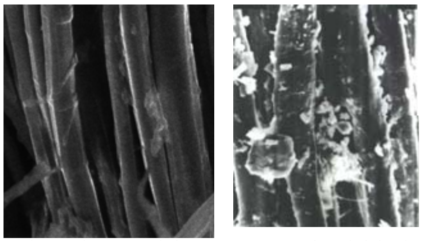

SEM images of : a) non-grafted reference linen support (1000x)

SEM Images: b) grafted (functionalized) reference linen (2300x)

***Fig. 2**. SEM images of:non-grafted reference linen support; grafted (functionalized) linen support.*

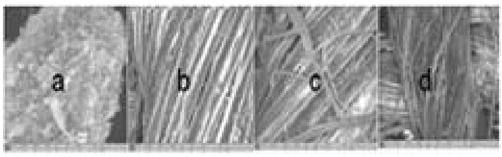

***Fig. 3**. SEM images of: a- ZnO powder hydrothermally synthesized; b–ZnO powder hydrothermally synthesized on grafted linen support (4_ ZnO (1200x)); c-ZnO powder hydrothermally synthesized on grafted linen support with assistance of Pluronic P123 (poly(ethylene glycol) (4_P123(1200x)); d-ZnO powder hydrothermally synthesized on grafted linen support with assistance of CTAB (Cetyltrimethylammoniumbromide) (4_CTAB (1200x)).*

As shown in Fig.4, the surfaces of the linen supports are very clear, with diameters of about 10-20 μm. This implies that the large particles may be formed via precipitation followed by a step-like aggregation process.

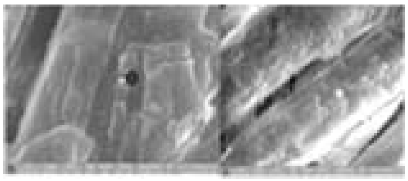

***Fig. 4**. SEM images of: e) ZnO powder hydrothermally synthesized on grafted linen support with assistance of CTAB (Cetyl trimethylammonium bromide) (4_CTAB (5000x)); f) ZnO powder hydrothermally synthesized on grafted linen support with assistance of Pluronic P123 (poly (ethylene glycol) (5000x) (4_P123).*

Due to its high number of coordinating functional groups (hydroxyl and glucoside groups) as polysaccharide, MCT-β-CD (monochlorotriazinyl–β-cyclodextrin) could form complexes with divalent metal ions [15]. It might be possible that the majority of the zinc ions was closely associated with the MCT-β-CD (monochlorotriazinyl–β-cyclodextrin) molecules. Based on the previous research, it can be claimed that nucleation and initial crystal growth of ZnO may preferentially occur on MCT-β-CD (monochlorotriazinyl–β-cyclodextrin). Moreover, as polysaccharide, MCT-β-CD (monochlorotriazinyl–β-Cyclodextrin) showed interesting dynamic supramolecular associations facilitated by inter- and intra-molecular hydrogen bonding, which could act as matrices for nanoparticle growth in size of about 30–40 nm. They aggregated to irregular ZnO–CMC nanoparticles in a further step. Figures 4e) and 4f) show SEM images of linen supports coated with ZnO with assistance of the two surfactants. As shown in the figures above, the nanoparticles exhibited an approximately lamellar morphology and the particles can be seen to be coated on the fibrous support surface. The fibrous supports surface became coarser after the treatment.

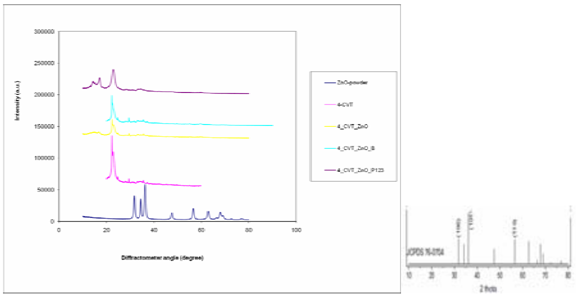

Fig. 5. *(Color online) XRD patterns of: ZnO-powder (ZnO non-calcinated powder hydrothermally synthesized); MCT- β -CD (Monochlorotriazinyl–β-cyclodextrin)* $_4$ *grafted (functionalized) linen fibrous support (4-CVT); ZnO powder hydrothermally synthesized on MCT-B-CD (Monochlorotriazinyl– β -Cyclodextrin)* $_4$ *grafted linen fibrous support (4_ZnO); ZnO powder hydrothermally synthesized on MCT-B-CD (Monochlorotriazinyl– β -Cyclodextrin)* $_4$ *grafted linen fibrous support in presence of Cetyl trimethylammonium bromide (4_CVT_ZnO_B)); ZnO powder hydrothermally synthesized on MCT-β-CD (Monochlorotriazinyl– β -Cyclodextrin)* $_4$ *grafted linen fibrous support in presence of P123 (4_CVT_ZnO_P123).*

In addition, according to the SEM images of the coated fabric, the uniformity of the fabric coated with ZnO powder hydrothermally synthesized with assistance of CTAB (Cetyl Trimethylammonium Bromide) is better than that of ZnO powder hydrothermally synthesized in the presence of Pluronic P123 and possesses good washing fastness. The coating particles fell off easily for the ZnO powder hydrothermally synthesized without any surfactant assistance after washing, which might have been caused by the weak attaching force (covalent bonding between ZnO and linen) induced by the deteriorated crystallinity.

The standard XRD pattern of ZnO - non-calcinated powder hydrothermally synthesized with hexagonal phase structure corresponds to JCPDS card No 76-0704 [16]. All peak positions and relatively very small, decreased peak intensities of ZnO–linen supports nanocomposites matched well with those of the standard XRD pattern, which confirms that the samples consist of ZnO on linen matrix without any other impurity phase.

As it can be seen in Fig. 5, the intensities of the diffraction peaks weaken as the FWHM of the peaks decreases with the assistance of the two surfactants. In the case of ZnO nanoparticles synthesized with the assistance of those two surfactants, the result is suppressed ZnO grain growth and deteriorated crystallinity; it can be noted that the width of the peaks for nano-ZnO fibrous composites has decreased in a more relevant manner, in case of the presence of P123, compared to the sample synthesis assisted by CTAB.

The diffraction peaks of ZnO–linen nanocomposites showed a broadening at the base due to the nano-size effect.

In Fig. 6, the *FTIR spectrum* of hydrothermally synthesized, non-calcinated ZnO powder exhibited a high intensity broad band at about 430 cm^{-1} due to the stretching of the zinc and oxygen bond.

A similar band was also observed in synthesized nano-ZnO composites. As shown in the FTIR spectrum of MCT-β-CD (Monochlorotriazinyl– β -Cyclodextrin) , the absorption bands between 1000 and 1200 cm^{-1} were characteristic of the – C –O– stretching on polysaccharide skeleton. And two peaks appeared at 1420 and 1610 cm^{-1} corresponding to the symmetrical and asymmetrical stretching vibrations of the carboxylate groups. And the peak at 2920 cm^{-1} was ascribed to C–H stretching associated with the ring methane hydrogen atoms. A broad band centered at 3450 cm^{-1} was attributed to a wide distribution of hydrogen-bonded hydroxyl groups. The FTIR spectra indicated that in ZnO–MCT-β-CD (Monochlorotriazinyl – β - Cyclodextrin) nanoparticles, there was the strong interaction, but no obvious formation of covalent bonds between MCT-β-CD (Monochlorotriazinyl – β - Cyclodextrin) and ZnO.

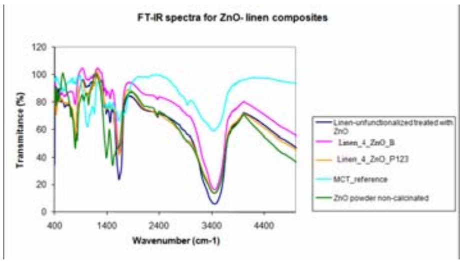

Fig. 6. *(a) FTIR of spectra of: linen fibrous – unfunctionalized and hydrothermally treated with ZnO (Linen unfuctionalized, hydrothermally treated with ZnO); the linen fibrous support grafted with MCT-β-CD (Monochlorotriazinyl– β -Cyclodextrin)$_4$ and hydrothermally treated with ZnO in presence of Cetyl trimethylammonium bromide (Linen_4_ZnO_B)); the linen fibrous support grafted with MCT-β-CD (Monochlorotriazinyl– β -Cyclodextrin)$_4$ and hydrothermally treated with ZnO in presence of P123 (Linen_4_ZnO_P123), MCT-β-CD (Monochlorotriazinyl– β -Cyclodextrin) powder (MCT-β-CD (Monochlorotriazinyl– β -Cyclodextrin) _reference), ZnO powder non-calcinated.*

The degradation efficiency, as a function of reaction time, was calculated considering the concentration ratio of the original solution and the ones of the analyzed samples (Eq.1) [17, 18].

$$\eta = (C_0 - C) \cdot 100/C_0 = (A_0 - A) \cdot 100/A_0 \quad (1),$$

where C_0 and A_0 are the initial concentration and absorbance of Erionyl Roth in solution at fixed wavelength, corresponding to the maximum absorption wavelength; C and A are the concentration and absorbance of the Erionyl Roth solution after UV light irradiation at different moments of time.

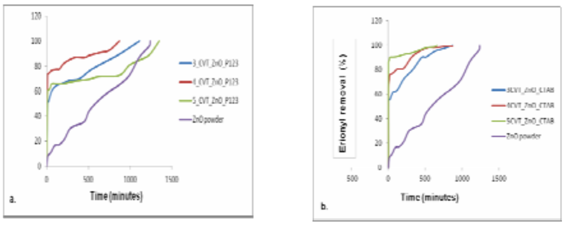

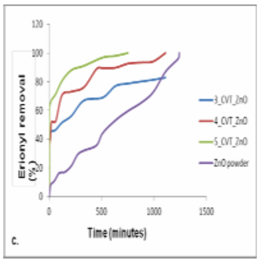

Fig.7.
Photocatalytic activity of the studied samples using 365 nm UV lamp.

Based on the photocatalytic experiments (Fig.7) using irradiation lamp at 365 nm, the following conclusions were drawn:

- 5_CVT_ZnO_CTAB>4_CVT_ZnO_CTAB>3 _CVT_ZnO_CTAB> ZnO powder;
- 5_CVT_ZnO>4_CVT_ZnO>ZnO powder >3 _CVT_ZnO;
- 4_CVT_ZnO_P123>3_CVT_ZnO_P123> 5_CVT_ZnO_P123> ZnO powder.

4. Conclusions

The ZnO nanoparticles were hydrothermally synthesized on linen fibrous supports having a different concentration of MCT-β-CD.The samples were characterized using co-assisted characterizing methods (RDX, SEM, FTIR). Comparing the two photocatalysts (with CTAB and P123) adsorption potential, it was found that the photocatalyst containing CTAB retained more than the one possessing P123. Among the probes containing CTAB as surfactant, the 5_CVT_ZnO_CTAB indexed sample is the best, in terms of photocatalytic activity.

Acknowledgments

The financial support provided by the Research Contract within POSDRU No. /89/1.5/S/49944 Project, belonging to “Al.I.Cuza” University of Iasi Authors is mentioned with gratitude.

References

[1]. **Hoffmann, M. R.; Martin, S. T.; Choi, W.; Bahnemann** - D. W. Chem. Rev. 1995, 95, 69–96.

[2]. **Tryba, B.; Morawski, A. W.; Tsumura, T.; Toyoda, M.; Inagaki, M. -** J. Photochem. Photobiol., A 2004, 167, 127–135.

[3]. **Li, Y. Z.; Song, J. S.; Lee, N.; Kim S.** - Langmuir 2004, 20, 10838–10844.

[4]. **Sun, B.; Smirniotis, P. G.; Boolchand, P.** - Langmuir 2005, 21, 11397–11403.

[5]. **Sakthivel, S.; Neppolian, B.; Shankar, M. V.; Arabindoo, B.; Palanichamy,M.; Murugesan, V.** - Sol. Energy Mater. Sol. Cells 2003, 77, 65–82.

[6]. **Khodja, A. A.; Sehili, T.; Pilichowski, J. F.; Boule, P**. - J. Photochem.Photobiol., A 2001, 141, 231–239.

[7]. **Sun, J. H.; Dong, S. Y.; Wang, Y. K.; Sun, S. P**. - J. Hazard. Mater. 2009, 172, 1520–1526.

[8]. **Yu, J. G.; Yu, X. X**. Environ. Sci. Technol. 2008, 42, 4902–4907.

[9]. **Ooka, C.; Yoshida, H.; Suzuki, K.; Hattori, T. -** Microporous Mesoporous Mater. 2004, 67, 143–150.

[10]. **Fukahori, S.; Ichiura, H.; Kitaoka, T.; Tanaka, H. -** Environ. Sci. Technol.2003, 37, 1048–1051.

[11]. **Zhang, G. K.; Ding, X. M.; He, F. S.; Yu, X. Y.; Zhou, J.; Hu, Y. J.; Xie, J. W**. - Langmuir 2008, 24, 1026–1030.

[12]. **Raveendran, P., Fu, J., Wallen, S.L.** - *Completely ‘‘green” synthesis and stabilization of metal nanoparticles,* J. Am. Chem. Soc. 125, 13940–13941 (2003)

[13]. **Vigneshwaran, N., Kumar, S., Kathe, A.A., Varadarajan, P.V., Prasad, V**. - *Functional finishing of cotton*

fabrics using zinc oxide–soluble starch nanocomposites, Nanotechnology 17, 5087–5095 (2006)

[14]. Ma, X.F., Chang, P.R., Yang, J.W., Yu, J.G. - *Preparation and properties of glycerol plasticized-pea starch/zinc oxide–starch bionanocomposites*, Carbohydr. Polym. 75, 472–478 (2009)

[15]. Radhakrishnan, T., Georges, M.K., Nair, P.S. - 2007. *Study of sago starch–CdS nanocomposite films: Fabrication, structure, optical and thermal properties,* J.Nanosci. Nanotechnol. 7, 986–993 (2007)

[16]. Jiugao, Yu, Jingwen, Yang, Baoxiang, Liu, Xiaofei, Ma - *Preparation and characterization of glycerol plasticized-pea starch/ZnO–carboxymethylcellulose sodium nanocomposites, Bioresource Technology* 100, 2832–2841 (2009)

[17]. F. Ollis, E. Pelizzetti, and N. Serpone - *“Photocatalyzed destruction of water contaminants,”* Environ. Sci.Tech., vol. 25, no. 9, pp. 1522-1529, Sept. 1991.

[18]. D. Y. Goswami - *“Engineering of the solar photocatalytic detoxification and disinfection processes,”* in Advances in Solar Energy, vol. 10,

[19]. K. W. Böer - Ed. Boulder: American Solar Energy Society Inc., 1995, pp.165-209.